Applied and Computational Harmonic Analysis **6,** 252–281 (1999)
Article ID acha.1998.0254, available online at http://www.idealibrary.com on IDEAL®

On the Time–Frequency Detection of Chirps[1]

Eric Chassande-Mottin and Patrick Flandrin

Laboratoire de Physique (URA 1325 CNRS), Ecole Normale Supérieure de Lyon, 46 allée d'Italie, 69364 Lyon Cedex 07, France

E-mail: echassan@physique.ens-lyon.fr; flandrin@physique.ens-lyon.fr

Communicated by Stephane G. Mallat

Received October 8, 1997; revised March 12, 1998

The question of detecting a chirp in the time–frequency plane is addressed. Strategies based on line integration are discussed with respect to optimality and adequacy of a representation to a given chirp. Linear and power-law chirps are considered in some detail and a possible application of affine distributions to the detection of gravitational waves is proposed, together with an effective implementation by means of reassigned spectrograms. © 1999 Academic Press

1. INTRODUCTION

Roughly speaking, "chirp" signals (or "chirps," for short) correspond to waveforms whose expression can be written in the time domain as

$$x(t) = a(t)e^{i\varphi(t)}, \tag{1}$$

with $a(t)$ some positive, low-pass, and smooth amplitude function whose evolution is slow as compared to the oscillations of the phase $\varphi(t)$. Defined this way, chirps are intended to serve as models for monocomponent signals modulated in both amplitude and frequency, their "instantaneous" frequency being assumed to be related to the "local" oscillations of the phase.

Chirps are ubiquitous in nature. They can be observed in animal communication (birds, frogs, whales, etc.) and echolocation (bats), geophysics (whistling atmospherics), astrophysics (gravitational waves radiated by coalescing binaries), acoustics (propagation of impulses in dispersive media), or biology (epileptic seizure activity in EEG data, uterine contractions in EMG, etc.). They are also extensively used in manmade systems, such as radar and sonar, or in the nondestructive evaluation of materials and seismic exploration.

[1] This work has been supported in part by CNRS (GdR-PRC ISIS and GREX). It was presented in part at the 4th World Congress of the Bernoulli Society, Vienna (Austria), August 1996.

1063-5203/99 $30.00

Copyright © 1999 by Academic Press
All rights of reproduction in any form reserved.

Intuitively, chirps $x(t)$ call for a time–frequency description in which a properly defined joint representation $\rho_x(t, f)$ should mainly exist—in the time–frequency plane—in a narrow neighborhood of a characteristic time–frequency curve $\mathcal{L}$, interpreted either as an "instantaneous frequency" (frequency as a function of time) or—from a dual perspective—as a "group delay" (time as a function of frequency). Assuming this holds, it therefore becomes very natural to propose heuristic schemes aimed at chirp detection by searching for such a time–frequency localization in a time–frequency distribution of an observation $r(t)$, e.g., by using as test statistics

$$\Lambda(r) = \int_{\mathcal{L}} \rho_r(t, f)$$

and comparing it to some threshold based on noise-only assumptions.

Moreover, in the case where the curve $\mathcal{L}$ also depends on some unknown vector of parameters θ, introducing the parameterized quantity

$$\Lambda(r; \theta) = \int_{\mathcal{L}(\theta)} \rho_r(t, f)$$

and looking for its maximum over θ should allow not only for the detection of $x(t)$ but also for the estimation of θ, such a strategy being reminiscent of a generalized Radon or Hough transform.

Beyond heuristic considerations, however, the rationale for using test statistics as above must be questioned and justified. In this respect, and for a given chirp to detect, three main questions have to be addressed:

1. Which time–frequency representation should be used to make sense of the idea of time-frequency localization?
2. How can a heuristic strategy based on some path integration in the time–frequency plane be made optimal in some precise statistical sense?
3. What can be gained from a time–frequency formulation of optimal chirp detection?

The two first questions are thoroughly addressed in this paper and, although the third one will not be considered in detail, the results reported here will provide the necessary hints for justifying the usefulness of a time–frequency reformulation of chirp detection, especially in terms of versatility and robustness. Special emphasis will be placed on the specific case of "power-law" chirps, because of their importance in the context of gravitational wave detection, but before proceeding to the power-law case, we will first introduce some definitions (Section 2) and begin the discussion with the more simple case of *linear* chirps, for which results have been known for a long time (Section 4). This will offer the guidelines for considering later desired generalizations to nonlinear situations such as power-law chirps (Section 5). Finally, a specific example related to the detection of gravitational waves expected to be radiated by coalescing binaries will be discussed and illustrated (Section 6).

It must be emphasized that the idea of using a time–frequency strategy for detecting

chirps is an old story and that various examples of application of such an approach have already been proposed in the literature, e.g., in [4, 5, 12, 13, 15, 25, 28] or, more recently, in [20, 21]. Moreover, many results which are needed for addressing the time–frequency detection problem have also been treated, *per se*, in the individual contexts of detection theory or time–frequency analysis (surveys can be found, e.g., in [8, 9, 14]). Most of them, however, will be recalled (or even restated) in the following, the main objective of the paper being to put together various ingredients and to combine them in a coherent fashion.

2. CHIRPS

Because of their great importance, chirps deserve, of course, a more precise and more rigorous definition than the one given above. A sophisticated mathematical treatment of chirps can be found in [22], whereas a discussion on the possibility of interpreting representations such as (1) in terms of instantaneous amplitude and frequency is given in [29]. We will not enter here, however, into the subtleties of both approaches and, when necessary, we will only make use of the following definitions:

DEFINITION 1. A signal $x(t)$ is said to be a chirp if it admits a representation as in (1), with $a(t)$ and $\varphi(t)$ such that

$$\left|\frac{\dot{a}(t)}{a(t)\dot{\varphi}(t)}\right| \ll 1$$

and

$$\left|\frac{\ddot{\varphi}(t)}{\dot{\varphi}^2(t)}\right| \ll 1,$$

where " $\dot{}$ " and " $\ddot{}$ " stand for the first and second derivatives, respectively.

The two conditions above aim at formalizing the idea of having fast oscillations under a slowly varying envelope. The first condition guarantees that, over a (local) pseudo-period $T(t) = 2\pi/\dot{\varphi}(t)$, the amplitude $a(t)$ experiences almost no relative change, whereas the second condition imposes that $T(t)$ itself is slowly varying, thus giving meaning to the notion of pseudo-period.

DEFINITION 2. A chirp $x(t)$ is said to be analytic if it is such that $\mathrm{Re}\{x(t)\}$ and $\mathrm{Im}\{x(t)\}$ form a Hilbert transform pair.

An equivalent characterization of analytic chirps amounts to saying that their spectrum is nonzero for positive frequencies only.

DEFINITION 3. Given an analytic chirp $x(t)$, the *instantaneous amplitude* $a_x(t)$ and *instantaneous frequency* $f_x(t)$ of $\mathrm{Re}\{x(t)\}$ are given, respectively, by $a_x(t) = |x(t)|$ and $f_x(t) = \dfrac{1}{2\pi}\dot{\varphi}(t)$.

DEFINITION 4. Given an analytic chirp $x(t)$, the *spectral envelope* $B_X(f)$ and *group delay* $t_X(f)$ of $\mathrm{Re}\{x(t)\}$ are given, respectively, by $B_X(f) = |X(f)|$ and $t_X(f) = -\frac{1}{2\pi}\dot{\Psi}(f)$, with $X(f)$ the Fourier transform of $x(t)$ and $\Psi(f)$ the phase of $X(f)$.[2]

Moreover, we will only consider *strictly monotonic chirps*, i.e., chirps such that the instantaneous frequency $f_x(t)$ and the group delay $t_X(f)$ are invertible functions.

Different types of chirps can be considered, depending on the form of $a(t)$ and/or $\varphi(t)$. We will adopt the following conventions:

DEFINITION 5. A chirp is said to be a *linear chirp* if it admits the representation (1) with $\varphi(t)$ a quadratic polynomial in t,

$$\varphi(t) = 2\pi\left(\frac{\alpha}{2}t^2 + \beta t + \gamma\right),$$

with α, β, and $\gamma \in \mathbf{R}$, and $\alpha \neq 0$.

It should be noted that, by construction, a linear chirp $x(t)$ defined this way has no reason to be analytic, with the consequence that the quantity $\frac{1}{2\pi}\dot{\varphi}(t) = \alpha t + \beta$ does not, in general, identify to the actual instantaneous frequency of the real-valued signal $\mathrm{Re}\{x(t)\}$. The actual conditions under which a linear chirp is almost analytic can be made precise in some cases, when an explicit model is given for the amplitude $a(t)$. In particular, in the important case of a Gaussian amplitude, we can easily prove that a linear chirp with a Gaussian amplitude $e^{-\pi\delta t^2}$ becomes almost analytic (i.e., almost vanishes for negative frequencies) in the narrow-band limit where $(\alpha^2 + \delta^2)/\delta\beta^2 \to 0$. This follows from a direct calculation according to which

$$|X(f)| = Ce^{-\pi(\delta/(\alpha^2+\delta^2))(f-\beta)^2}.$$

We get from this result that the central frequency of a chirp with a Gaussian amplitude is β, whereas its bandwidth is proportional to $(\delta + \alpha^2/\delta)^{1/2}$, whence the narrow-band condition.

The situation of quasi-analyticity of linear chirps contrasts with that of *power-law* chirps, which are analytic by construction and whose definition is the following:

DEFINITION 6. A chirp is said to be a power-law chirp (of indices $r \in \mathbf{R}$ and $k \leq 0$) if its spectrum is nonzero for positive frequencies only and if it admits the frequency representation

$$X_{r,k}(f) = Cf^{-(r+1)}e^{i\Psi_k(f)}U(f), \tag{2}$$

[2] Throughout the paper, we will adopt the convention of using a lower case symbol for representing a quantity in the time domain and the corresponding upper case symbol for denoting its Fourier transform, in the frequency domain.

with $\Psi_k(f) = -2\pi(cf^k + t_0 f + \gamma)$ if $k < 0$, $\Psi_0(f) = -2\pi(c \log f + t_0 f + \gamma)$, C, c, t_0, $\gamma \in \mathbf{R}$ and where $U(\cdot)$ stands for the unit step function.

A power-law chirp therefore is characterized by a group delay of the form $t_X(f) = t_0 + ckf^{k-1}$. Although the definition could be extended to positive k's, we will restrict ourselves in the following to the case $k \leq 0$, for which the group delay corresponds to some generalized hyperbola in the time-frequency plane.

3. DETECTION

3.1. Optimum Detection

Signal detection is usually considered from the point of view of the binary hypothesis testing problem (see, e.g., [37])

$$H_0\colon r(t) = n(t)$$

$$H_1\colon r(t) = n(t) + s(t),$$

with $-T/2 \leq t \leq T/2$, and where $s(t)$ is the reference signal to detect (supposed to be known and of finite energy over $[-T/2, T/2]$), $n(t)$ is some additive noise, and $r(t)$ is the available observation upon which the decision has to be taken.

Given this framework, designing an "optimal" detector depends not only on the *a priori* knowledge one may have on the signal and on the noise, but also on the choice of a criterion for optimality. A relevant concept in such a search for optimality is that of the "likelihood ratio test" (LRT), which essentially consists in evaluating the test statistics

$$\lambda(r) = \frac{p_1(r)}{p_0(r)},$$

where $p_0(r)$ and $p_1(r)$ stand for the conditional probability density functions of the observation under H_0 and H_1, respectively. Once the LRT is computed, the detection itself amounts to comparing it with a threshold and to deciding that the expected signal is indeed present when the threshold is exceeded.

We are interested here in the case where the expected signal expresses as

$$s(t) = x(t;\, \theta)e^{i\gamma},$$

where θ is a vector of unknown parameters that we may wish to estimate, and γ some unknown random phase, uniformly distributed over $[0, 2\pi]$, that we would like to eliminate. In such a situation, the notion of LRT must be extended to that of generalized LRT (GLRT), defined as

$$\tilde{\lambda}(r;\, \theta) = \frac{1}{2\pi} \frac{\int_0^{2\pi} p_1(r|\gamma)d\gamma}{p_0(r)}.$$

Given this modified test statistics, detection is still based on a comparison with a threshold, and (maximum likelihood) estimation can be simultaneously achieved according to

$$\hat{\theta} = \arg\max_{\theta} \tilde{\lambda}(r;\, \theta).$$

In order to get an explicit form for the GLRT, some further assumptions are necessary about the statistics of the additive noise. For the sake of simplicity, $n(t)$ will be assumed to be zero-mean, Gaussian, and white, i.e., such that

$$\mathbf{E}\{n(t)\overline{n(s)}\} = N_0\delta(t-s)$$

for any t and s in **R,** with $\mathbf{E}\{\cdot\}$ the expectation operator. Such an assumption allows for simplifications in the writing of the GLRT, since we have [37]

$$\frac{p_1(r|\gamma)}{p_0(r)} = \exp\left\{-\frac{1}{N_0}\int_{-T/2}^{T/2}(|r(t)-x(t;\,\theta)e^{i\gamma}|^2 - |r(t)|^2)dt\right\}.$$

After some manipulations, the GLRT follows as

$$\tilde{\lambda}(r;\,\theta) = e^{-E_x(\theta)/2N_0}\frac{1}{2\pi}\int_0^{2\pi}\exp\left\{\frac{1}{N_0}(F(\theta)e^{-i\gamma} + \overline{F(\theta)}e^{i\gamma})\right\}d\gamma,$$

with $E_x(\theta)$ the signal energy and

$$F(\theta) = \int_{-T/2}^{T/2} r(t)\overline{x(t;\,\theta)}dt.$$

Expressing the above quantity in polar form as $F(\theta) = |F(\theta)|e^{i\varphi_F(\theta)}$ and reorganizing terms, we are led to

$$\tilde{\lambda}(r;\,\theta) = e^{-E_x(\theta)/2N_0}\frac{1}{2\pi}\int_0^{2\pi}\exp\left\{\frac{2|F(\theta)|}{N_0}\cos(\varphi_F(\theta)-\gamma)\right\}d\gamma,$$

a result which can be rewritten as

$$\tilde{\lambda}(r;\,\theta) = e^{-E_x(\theta)/2N_0}I_0\left(\frac{2|F(\theta)|}{N_0}\right),$$

where $I_0(\cdot)$ is the modified Bessel function of first kind [1].

The remarkable point is that, $I_0(\cdot)$ being a monotonic increasing function, the test statistics reduces to compare $|F(\theta)|$ (or any monotonic increasing function of $|F(\theta)|$) with

a threshold. It follows therefore that the basic ingredient for the considered GLRT detection may simply reduce to

$$\Lambda(r;\,\theta) = \left| \int_{-T/2}^{T/2} r(t)\overline{x(t;\,\theta)}dt \right|^2.$$

Concerning estimation, however, some care must be taken since maximizing over θ the simplified statistics $\Lambda(r;\,\theta)$ in place of the exact one $\tilde{\lambda}(r;\,\theta)$ implicitly assumes that the signal energy $E_x(\theta)$ does not depend upon θ.

The strategy invoked here is exceedingly simple, since it only amounts to correlating the observation with a replica of the expected waveform, but one should not forget that this is so because of the many assumptions which have been made, especially that of Gaussianity. As far as interpretation is concerned, one can note that the GLRT detector admits a companion interpretation in terms of "matched filtering," a concept based on the idea of filtering the observation in such a way that the signal-to-noise ratio (i.e., the contrast between the two competing hypotheses) is maximized at the output of the filter. Because of the corrupting random phase, the optimum GLRT detector turns out to coincide with a matched filter followed by an envelope detector, a structure referred to as "quadrature matched filtering [37]."

Until now, the additive noise has been assumed to be white. In the more realistic situation where the noise, while stationary and zero-mean, is colored, the same strategy can still be applied, *mutatis mutandis,* under the assumption of Gaussianity, provided that the observation must first be whitened. More precisely, and provided that the time support of the signal to detect is entirely contained in the observation interval $[-T/2,\ T/2]$, Parseval's relation guarantees that

$$\left| \int_{-T/2}^{T/2} r(t)\overline{x(t;\,\theta)}dt \right|^2 = \left| \int_0^{+\infty} R(f)\overline{X(f;\,\theta)}df \right|^2$$

for analytic signals. Therefore, if we introduce the whitening operation

$$x(t) \rightarrow x^w(t) = \int_0^{+\infty} \frac{X(f)}{\sqrt{\Gamma_n(f)}}\, e^{i2\pi ft}df,$$

and if we apply this to the observation, the problem of detecting a given signal in colored noise is (at least formally) transformed into a new problem of detecting a prefiltered version of the original signal in white noise, thus leading to the following strategy:

$$\Lambda^w(r;\,\theta) = \left| \int_0^{+\infty} \frac{R(f)\overline{X(f;\,\theta)}}{\Gamma_n(f)}\, df \right|^2. \tag{3}$$

It is basically this quantity which has to be given an equivalent time–frequency formulation.

3.2. Time–Frequency Detection

As shown by the structure of the GLRT, optimum detection relies on a correlation measure—in terms of the squared inner product—between the observation and a reference. This correlation can be expressed equivalently in the time domain or in the frequency domain, and this naturally suggests that a third equivalent approach should be feasible, in which the inner product would be directly written in time and frequency (i.e., jointly) by means of a suitable time–frequency distribution which can be thought of as a "signature" well adapted to nonstationary signals.

The idea, therefore, is to introduce such a time–frequency distribution $\rho_x(t, f)$ (which necessarily must be at least quadratic in x) so that we may have, for any signals $x_1(t)$ and $x_2(t)$, a relation of the type

$$|\langle x_1, x_2\rangle_t|^2 = |\langle X_1, X_2\rangle_f|^2 = \langle\langle \rho_{x_1}, \rho_{x_2}\rangle\rangle_{tf},$$

where $\langle \cdot, \cdot \rangle_t$, $\langle \cdot, \cdot \rangle_f$, and $\langle\langle \cdot, \cdot \rangle\rangle_{tf}$ stand for suitably chosen inner products in the time domain, the frequency domain, and the time–frequency domain, respectively (explicit definitions of such inner products will be detailed in the following for giving a precise meaning to the above equalities).

Such an equivalence obviously has no reason to hold for any quadratic time–frequency distribution. For instance, it is not verified by the simplest distributions we may think of, namely the *spectrogram* (squared short-time Fourier transform) and the *scalogram* (squared wavelet transform). This can be checked by direct inspection, but this claim (and, with it, the way to find suitable distributions which overcome the limitations of spectrograms and scalograms) can be justified in a more interesting manner by considering general classes of distributions to which spectrograms and scalograms belong. We can introduce, for instance, the following definition [9, 14]:

DEFINITION 7. The class of all quadratic time–frequency distributions which are covariant with respect to shifts in time and frequency is referred to as *Cohen's class* and reads

$$C_x^{(\varphi)}(t, f) = \int \int_{-\infty}^{+\infty} \varphi(\xi, \tau) A_x(\xi, \tau) e^{-i2\pi(\xi t + \tau f)} d\xi d\tau,$$

with

$$A_x(\xi, \tau) = \int_{-\infty}^{+\infty} x\left(t + \frac{\tau}{2}\right) \overline{x\left(t - \frac{\tau}{2}\right)} e^{i2\pi\xi t} dt$$

and where $\varphi(\xi, \tau)$ is some arbitrary parameterization function such that $\varphi(0, 0) = 1$.

With this definition, it is easy to establish the following result [23]:

PROPOSITION 1. *A time–frequency distribution belonging to Cohen's class is* unitary, *i.e., satisfies*

$$\left| \int_{-\infty}^{+\infty} x_1(t)\overline{x_2(t)}dt \right|^2 = \int \int_{-\infty}^{+\infty} C_{x_1}^{(\varphi)}(t, f)\overline{C_{x_2}^{(\varphi)}(t, f)}dtdf,$$

if and only if the arbitrary parameterization function $\varphi(\xi, \tau)$ *is of modulus unity.*

The consequence of this result is that a spectrogram with window h cannot be unitary since it is well known [9, 14] that it belongs to Cohen's class with $\varphi(\xi, \tau) = \overline{A_h(\xi, \tau)}$, a quantity which cannot be of modulus unity over the entire (ξ, τ) plane. A similar result can be established for scalograms, which are known to be members of the so-called *affine* class [14]. It appears, therefore, that those distributions (spectrogram and scalograms) are *a priori* not qualified for serving as the basis of an *optimum* time–frequency detector, although they may have been put forward for this purpose and may have proven useful as suboptimum detectors [2, 20, 21]. Other distributions can be found, however, which are optimal with respect to detection. Whereas the interested reader is referred, e.g., to [13, 31] for a general discussion about optimum time–frequency detection, we will focus here on the specific case of chirp detection.

4. DETECTING LINEAR CHIRPS

The optimum time–frequency detection of linear chirps was first considered in [25]. From a time–frequency perspective, it turns out that linear chirps are intimately related to a special member of Cohen's class, the so-called Wigner–Ville distribution, defined as follows [9, 14]:

DEFINITION 8. The *Wigner–Ville distribution* of a signal $x(t)$ is the special case of Cohen's class attached to the parameterization $\varphi(\xi, \tau) = 1$, and its (real-valued) expression reads explicitly

$$W_x(t, f) = \int_{-\infty}^{+\infty} x\left(t + \frac{\tau}{2}\right)\overline{x\left(t - \frac{\tau}{2}\right)}e^{-i2\pi f\tau}d\tau. \tag{4}$$

The reason that linear chirps and the Wigner–Ville distribution are closely linked together is given by the following

PROPOSITION 2. *When applied to the linear chirp of Definition* 5, *with* $a(t) = 1$, *the Wigner–Ville distribution* (4) *is perfectly localized and reads*

$$W_x(t, f) = \delta\left(f - \frac{1}{2\pi}\dot{\varphi}(t)\right).$$

Since the parameterization function of the Wigner–Ville distribution is $\varphi(\xi, \tau) = 1$, it is of course of modulus unity, thus guaranteeing unitarity. It follows, therefore, that we have

$$\left| \int_{-\infty}^{+\infty} x_1(t)\overline{x_2(t)}dt \right|^2 = \int \int_{-\infty}^{+\infty} W_{x_1}(t, f)W_{x_2}(t, f)dtdf$$

for any two signals $x_1(t)$ and $x_2(t)$. In the case where $x_1(t) = r(t)\mathbf{1}_{[-T/2,T/2]}$ (with $\mathbf{1}_I(t)$ the indicator function of the interval I) and where $x_2(t)$ is the linear chirp $x_2(t) = a(t)e^{i(\varphi(t)-2\pi\gamma)}$, we get (thanks to the support-preserving property of the Wigner–Ville distribution and its compatibility with modulations [9, 14])

$$\left| \int_{-T/2}^{T/2} r(t)a(t)e^{i(\varphi(t)-2\pi\gamma)}dt \right|^2 = \int_{-T/2}^{T/2} \int_{-\infty}^{+\infty} W_{r,a}(t, f)\delta\left(f - \frac{1}{2\pi}\dot{\varphi}(t)\right)dtdf$$

$$= \int_{-T/2}^{T/2} \left(\int_{-\infty}^{+\infty} W_a\left(t, \frac{1}{2\pi}\dot{\varphi}(t) - \xi\right)W_r(t, \xi)d\xi \right)dt.$$

It follows, therefore, that the GLRT optimum detection (in zero-mean white Gaussian noise) of a linear chirp with unknown parameters $\theta = (\alpha, \beta)$ can be achieved by using as test statistics the time–frequency-based quantity

$$\Lambda(r; \alpha, \beta) = \int_{-T/2}^{T/2} \rho_r(t, \alpha t + \beta)dt,$$

with

$$\rho_r(t, f) = \int_{-\infty}^{+\infty} W_a(t, f - \xi)W_r(t, \xi)d\xi.$$

Given the linear chirp model (5), the energy of the signal to detect does not depend upon the unknown parameters α and β, thus allowing for their maximum likelihood estimation *via* $\Lambda(r; \alpha, \beta)$.

5. DETECTING POWER-LAW CHIRPS

In the case of power-law chirps, the Wigner–Ville distributions is no longer a good candidate since, although unitary, it lacks the localization property which permits us to come up with a solution in terms of a path integral. In the specific case of hyperbolic chirps (i.e., $k = 0$), a well-adapted solution has been proposed in [28] on the basis of a variant of the Wigner–Ville distribution (the so-called Altes–Marinovic distribution), obtained from it by means of a warping operation. We will not follow this approach here because of two different shortcominings, namely the fact that the resulting strategy is not shift invariant in time (which may be a problem if the time origin of the chirp is unknown and has to be estimated) and also that the technique developed for the case $k = 0$ cannot be directly extended to arbitrary (negative) k's.

The framework we rather propose to use is that of *affine time–frequency distributions,*

as developed by J. and P. Bertrand [6]. Those distributions form a whole class of time–frequency distributions but, as compared to the previously introduced Cohen's class, their introduction is motivated by a covariance requirement with respect to each solvable three-parameter extension of the affine group. The effective construction results in a parameterized family of distributions for which we will adopt the following definition [6]:

DEFINITION 9. The *Bertrand distribution* (of index $k \in \mathbf{R}$) of an analytic signal $X(f)$ is given by

$$P_X^{(k)}(t, f) = f^{2(r+1)-q} \int_{-\infty}^{+\infty} \mu_k(u)\, X(f\lambda_k(u))\overline{X(f\lambda_k(-u))} e^{i2\pi t f \zeta_k(u)} du, \tag{5}$$

with

$$\zeta_k(u) = \lambda_k(u) - \lambda_k(-u).$$

In this definition, r and q are free real-valued parameters and $\mu_k(u)$ is some arbitrary function, whereas the explicit form of the parameterization function $\lambda_k(u)$ is fixed by

$$\lambda_k(u) = \left(k \frac{e^{-u} - 1}{e^{-ku} - 1} \right)^{1/(k-1)}$$

if $k \neq 0, 1$, the special cases attached to $k = 0$ and $k = 1$ being defined by continuity as

$$\lambda_0(u) = \frac{u}{1 - e^{-u}}$$

and

$$\lambda_1(u) = \exp\left(1 + \frac{u e^{-u}}{e^{-u} - 1} \right).$$

One can note that a Bertrand distribution is real valued if we have the hermitian symmetry condition $\mu_k(u) = \overline{\mu_k(-u)}$, a condition we will assume to be satisfied in the following.

In order to derive the time–frequency formulation of the power-law chirp detector, we will need a few results about Bertrand distributions. We will summarize this material in the following Propositions 3 to 6, whose proofs can be found in [6, 7].

Localization—Whereas the Wigner–Ville distribution was naturally adapted to linear chirps, the adequacy between Bertrand distributions and power-law chirps is shown by the following proposition [6]:

PROPOSITION 3. *When applied to the power-law chirp* (2), *the Bertrand distribution of index k* (5) *is* perfectly localized *on the group delay curve* $t_X(f) = t_0 + ck f^{k-1}$ *and reads*

$$P^{(k)}_{X_{r,k}}(t, f) = C^2 f^{-(q+1)} \delta(t - t_X(f)), \tag{6}$$

if and only if the arbitrary weighting function $\mu_k(u)$ *is given by*

$$\mu_k(u) = \dot{\zeta}_k(u)(\lambda_k(u)\lambda_k(-u))^{r+1}.$$

This proves that, in terms of time–frequency localization, the structure of Bertrand distributions is matched to that of power-law chirps, which constitutes the first ingredient for time–frequency detection *via* path integration.

Filtering—When leaving the class of power law chirps, the Bertrand distribution is no longer perfectly localized. For example, when a signal is filtered, the following proposition evidences that its Bertrand distribution filtered accordingly. More precisely [7]:

PROPOSITION 4. *When applied to a product signal* $X(f) = M(f)Y(f)$, *the Bertrand distribution* $P^{(k)}_X(t, f)$ *reads*

$$P^{(k)}_X(t, f) = f^{q+1} \int_{-\infty}^{+\infty} P^{(k)}_{M_r}(t - \theta, f) P^{(k)}_Y(\theta, f) d\theta,$$

where

$$M_r(f) = f^{-(r+1)} M(f).$$

Unitarity—The third ingredient we will need is unitarity, for which—introducing suitable inner products on the half-line of positive frequencies and on the associated time–frequency half-plane—we have the following result [6]:

PROPOSITION 5. *A Bertrand distribution is* unitary, *i.e., satisfies*

$$\left| \int_0^{+\infty} X(f)\overline{Y(f)} f^{2r+1} df \right|^2 = \int_{-\infty}^{+\infty} \int_0^{+\infty} P^{(k)}_X(t, f) P^{(k)}_Y(t, f) f^{2q} dt df$$

for any two signals $X(f)$ *and* $Y(f)$, *if and only if the arbitrary weighting function* $\mu_k(u)$ *is given by*

$$\mu_k(u) = \dot{\zeta}^{1/2}_k(u)(\lambda_k(u)\lambda_k(-u))^{r+1}.$$

Extended unitarity—As a corollary to Propositions 3 and 5, the requirements of localization and unitarity can be simultaneously fulfilled only if $\dot{\zeta}_k(u) = 1$, an equation whose only solution in k is $k = 0$ (this can readily be established by noting that we have the relation $\lambda_k(u) = e^u \lambda_k(-u)$, for any k [6]). Unless we want to consider only the case of hyperbolic chirps, it seems, therefore, that the two properties of localization and unitarity cannot be combined directly, so as to mimic what had been done previously in

the case of linear chirps. A way out, however, is possible, which relies on the following proposition [6]:

PROPOSITION 6. *Given a localized Bertrand distribution* $P_X^{(k)}(t, f)$ *with* $k < 0$, *there exists an auxiliary distribution* $\tilde{P}_X^{(k)}(t, f)$ *characterized by*

$$\tilde{\mu}_k(u) = (\lambda_k(u)\lambda_k(-u))^{r+1}$$

and such that

$$\left| \int_0^{+\infty} X(f)\overline{Y(f)}f^{2r+1}df \right|^2 = \int_{-\infty}^{+\infty} \int_0^{+\infty} \tilde{P}_X^{(k)}(t, f)\, P_Y^{(k)}(t, f)\, f^{2q}dtdf$$

for any two signals $X(f)$ *and* $Y(f)$.

This offers some additional freedom in the manipulation of Bertrand distributions, by softening the strict constraint of unitarity attached to one given distribution *via* the introduction of a pair of distributions and a duality relation between them. In the specific case $k = -1$, this duality identifies to a situation considered by Unterberger (see [36]), who coined the terms "active" and "passive" for distinguishing the corresponding distributions. As a generalization, we will therefore adopt the following definiton:

DEFINITION 10. The auxiliary distribution $\tilde{P}_X^{(k)}(t, f)$ is called the *passive* distribution associated with $P_X^{(k)}(t, f)$, the latter being referred to as *active.*

Although, by construction, the passive form of a distribution lacks the localization property of its associated active form, the former can be explicitly related to the latter, as shown by the following proposition:

PROPOSITION 7. *The passive form* $\tilde{P}_X^{(k)}(t, f)$ *of a localized Bertrand distribution is related to the corresponding active form* $P_X^{(k)}(t, f)$ *by*

$$\tilde{P}_X^{(k)}(t, f) = f \int_{-\infty}^{+\infty} G_k(f(t - \theta))\, P_X^{(k)}(\theta, f)d\theta,$$

where

$$G_k(s) = \int_{-\infty}^{+\infty} e^{i2\pi s\zeta_k(u)}du.$$

Proof. Starting from the definition of the passive distribution, based on the weighting function $\tilde{\mu}_k(u)$, we can write

$$\tilde{P}_X^{(k)}(t,f) = f^{2(r+1)-q}\int_{-\infty}^{+\infty} \tilde{\mu}_k(u)\, X(f\lambda_k(u))\overline{X(f\lambda_k(-u))}e^{i2\pi t f\zeta_k(u)}du$$

$$= f^{2(r+1)-q}\int_{-\infty}^{+\infty} \frac{\tilde{\mu}_k(u)}{\mu_k(u)}\,[\mu_k(u)\, X(f\lambda_k(u))\overline{X(f\lambda_k(-u))}]e^{i2\pi t f\zeta_k(u)}du$$

$$= \int_{-\infty}^{+\infty} \frac{f^{2(r+1)-q}}{\dot{\zeta}_k(u)}\,[\mu_k(u)\, X(f\lambda_k(u))\overline{X(f\lambda_k(-u))}]e^{i2\pi t f\zeta_k(u)}du,$$

so as to make appear explicitly the weighting function $\mu_k(u)$ of the associated active distribution. Using then the fact that, for $k \leq 0$, the function $\zeta_k(u) = \lambda_k(u) - \lambda_k(-u)$ is one-to-one from **R** to **R,** one can make the change of variable $u = \zeta_k^{-1}(v)$ in order to express $\tilde{P}_X^{(k)}(t,f)$ as an ordinary Fourier transform. We get, therefore,

$$\tilde{P}_X^{(k)}(t,f) = \int_{-\infty}^{+\infty} \frac{f^{2(r+1)-q}}{\dot{\zeta}_k(\zeta_k^{-1}(v))}\left[\frac{\mu_k(\zeta_k^{-1}(v))}{\dot{\zeta}_k(\zeta_k^{-1}(v))}\, X(f\lambda_k(\zeta_k^{-1}(v)))\overline{X(f\lambda_k(-\zeta_k^{-1}(v)))}\right]e^{i2\pi t f v}dv$$

$$= \int_{-\infty}^{+\infty} G_k(s)\, P_X^{(k)}\left(t-\frac{s}{f},f\right)ds = f\int_{-\infty}^{+\infty} G_k(f(t-\theta))\, P_X^{(k)}(\theta,f)d\theta,$$

with

$$G_k(s) = \int_{-\infty}^{+\infty} \frac{1}{\dot{\zeta}_k(\zeta_k^{-1}(v))}\, e^{i2\pi s v}dv$$

$$= \int_{-\infty}^{+\infty} \frac{d}{dv}\,(\zeta_k^{-1}(v))e^{i2\pi s v}dv$$

$$= \int_{-\infty}^{+\infty} e^{i2\pi s\zeta_k(u)}du,$$

whence the result follows.

Given an active distribution, its passive counterpart appears, therefore, as a filtered version of it in time, the impulse response G_k of the filter being frequency dependent (the equivalent "width," in time, of G_k varies as the inverse of frequency). In the general case (arbitrary k), no closed form expression exists for G_k. Let us note, however, that in the case where $k = -1$ ($\lambda_{-1}(u) = e^{u/2}$, Unterberger distribution [6]), we get explicitly

$$G_{-1}(s) = \int_{-\infty}^{+\infty} \frac{1}{\sqrt{1+v^2/4}}\, e^{i2\pi s v}dv \;= 4K_0(4\pi|s|),$$

where $K_0(\cdot)$ is the modified Bessel function of second kind [1], in accordance with the results given in [36].

All the different results derived so far can now be combined together and lead to the following central result:

PROPOSITION 8. *Given the detection problem where the signal $x(t;\,\theta_0)$ to detect is the power-law chirp* (2) *of group delay $t_X(f) = t_0 + c_0 k f^{k-1}$ with unknown parameters $\theta_0 = (t_0,\, c_0)$, and where the additive noise $n(t)$ is Gaussian, zero-mean, and stationary with power spectral density $\Gamma_n(f)$, the optimum test statistics admits the equivalent time–frequency formulation*

$$\Lambda^w(r;\,t,\,c) = \int_0^{+\infty} \rho_R(t + ckf^{k-1},\, f)\,df, \tag{7}$$

with

$$\rho_R(t,\,f) = C^2 f^{2q} \int_{-\infty}^{+\infty} \tilde{P}_A^{(k)}(t - s,\,f)\, P_R^{(k)}(s,\,f)\,ds \tag{8}$$

and

$$A(f) = \frac{f^{-(3r+2)}}{\Gamma_n(f)}\, U(f). \tag{9}$$

Proof. Let us first assume that $\theta_0 = (t_0,\, c_0)$ is known. In this case, starting from the results of Propositions 3 (localization) and 6 (extended unitarity), we readily obtain [6], for any signal $Z(f)$

$$\left| \int_0^{+\infty} Z(f)\overline{X_{r,k}(f)} f^{2r+1}\,df \right|^2 = \int_{-\infty}^{+\infty} \int_0^{+\infty} \tilde{P}_Z^{(k)}(t,\,f)\, P_{X_{r,k}}^{(k)}(t,\,f)\, f^{2q}\,dt\,df$$

$$= C^2 \int_0^{+\infty} \tilde{P}_Z^{(k)}(t_X(f),\,f)\, f^{q-1}\,df.$$

It follows, therefore, that the left-hand side of the above equation exactly identifies with the test statistics (3) if $Z(f) = R(f)\, f^{-(2r+1)}/\Gamma_n(f)$ and $X(f;\,\theta_0) = X_{r,k}(f)$. As a consequence, the right-hand side of the same equation provides an alternate time–frequency formulation for the power-law chirp detection problem and, making use of the results established in Proposition 4 (filtering), we end up with the claimed result, with $\theta = \theta_0$, i.e., $t = t_0$ and $c = c_0$. In the actual case where the parameter vector θ_0 is unknown, the same statistics must be used by replacing θ_0 with a set of test values $\theta = (t,\, c)$. Detection is then achieved when

$$\max_{(t,c)} \Lambda^w(r;\,t,\,c) > \eta,$$

where η is some prescribed threshold, while estimation of θ_0 can be carried out according to

$$\hat{\theta}_0 = (\hat{t}_0, \hat{c}_0) = \arg\max_{(t,c)} \Lambda^w(r; t, c).$$

According to this result, power-law chirps embedded in Gaussian noise can be optimally detected *via* a path integration strategy in the time–frequency plane, and their parameters can be estimated by means of a generalized Radon or Hough transform applied to a well-defined distribution. A potential application of this result will now be discussed.

6. THE EXAMPLE OF GRAVITATIONAL WAVES

Whereas the existence of gravitational waves was predicted long ago by general relativity theory, no direct experimental evidence has yet been obtained. Detecting gravitational waves on earth is very challenging because of the extremely tiny effects they induce on physical systems, and it is only in the very recent past that projects at the front end of current technologies may have been launched. In both VIRGO and LIGO projects—the main projects, which are still under construction—the detector is basically a giant laser interferometer, expected to convert the impinging of a gravitational wave into a detectable motion of interference fringes. Because gravitational waves are so weak, and although the interferometers have arms more than 3 km long, detectability requires a relative sensitivity of the order of 10^{-22}. Given the noise limitations of the detectors, this, however, should be possible in a frequency "window" between a few tenths and a few hundreds of Hertz.

As far as detection itself is concerned (from a signal processing point of view), a key question is to get some *a priori* information about possible structures for the expected waveforms. In fact, a wide variety of situations can be considered [32], each corresponding to different types of signals, more or less well characterized. Nevertheless, it is somewhat universally accepted that the most promising source of detectable gravitational waves should be produced by the coalescence of very massive binary systems, the only situation we will consider here.

6.1. A Model for Coalescing Binaries

A "coalescing binary" is a system of two very massive astrophysical objects (e.g., neutron stars or black holes), rotating around each other. In the process of this rotation, some gravitational energy is radiated in the form of gravitational waves, with the consequence that the objects become closer and closer, thus speeding up the rotation, up to coalescence. It intuitively follows that coalescing binaries should naturally give rise to gravitational waves which behave as chirps.

In a first (Newtonian) approximation, an explicit form can be given for the expected waveform. Up to some unknown phase, it can be expressed as the real part of the complex-valued signal [30, 34]

$$x(t; t_0, d) = A(t_0 - t)^{-\alpha} e^{-i2\pi d(t_0 - t)^{\beta}} U(t_0 - t), \tag{10}$$

with $\alpha = \frac{1}{4}$ and $\beta = \frac{5}{8}$. In this expression, t_0 is the coalescence time, and d and A are constants which mainly depend on the individual masses of the objects and, of course, of other geometrical quantities such as the distance of the binary from earth or the relative orientation between the wavefronts and the detector. More precisely, given two objects of individual masses m_1 and m_2, one can introduce the "total mass" $M = m_1 + m_2$ and the "reduced mass" μ such that $\mu^{-1} = m_1^{-1} + m_2^{-1}$. Using these two quantities, one can then define [34] the "chirp mass" $\mathcal{M} = \mu^{3/5} M^{2/5}$ and, following [30], we have

$$d = 160 \times 3^{3/8} \mathcal{M}_\odot^{-5/8} \approx 241 \mathcal{M}_\odot^{-5/8},$$

with $\mathcal{M}_\odot = \mathcal{M}/M_\odot$ and where $M_\odot$ stands for the solar mass. For an optimal relative orientation between the detector and the binary, we have furthermore [26]

$$A = \left(\frac{4}{3^{3/4}}\right) 1.92 \times 10^{-21} \frac{\mathcal{M}_\odot^{5/4}}{r} \approx 3.37 \times 10^{-21} \frac{\mathcal{M}_\odot^{5/4}}{r},$$

where r is the earth–binary distance, expressed in Mpc.

According to Definition 1, the waveform (10) can thus be interpreted as a chirp if the amplitude $a(t) = (t_0 - t)^{-\alpha}$ and the phase $\varphi(t) = 2\pi d (t_0 - t)^{\beta}$ are such that

$$\left| \frac{\dot{a}(t)}{a(t)\dot{\varphi}(t)} \right| = \frac{\alpha}{2\pi d \beta} (t_0 - t)^{-\beta} \ll 1$$

and

$$\left| \frac{\ddot{\varphi}(t)}{\dot{\varphi}^2(t)} \right| = \frac{|\beta - 1|}{2\pi d \beta} (t_0 - t)^{-\beta} \ll 1.$$

As mentioned in [11], these two conditions lead to one single condition according to which the model (10) can be given a chirp interpretation over the time interval characterized by

$$t_0 - t \gg t_c = \left(\frac{\max\{\alpha, |\beta - 1|\}}{2\pi d \beta} \right)^{1/\beta}. \tag{11}$$

In the specific case of gravitational waves, it follows from the values of the different constants that we have

$$t_c = 3 \times (1600\pi)^{-8/5} \mathcal{M}_\odot \approx 3.6 \times 10^{-6} \mathcal{M}_\odot.$$

Assuming that the chirp interpretation is valid, the waveform (10) has (approximately) for instantaneous frequency

$$f_x(t) = \frac{5d}{8} (t_0 - t)^{-3/8}$$

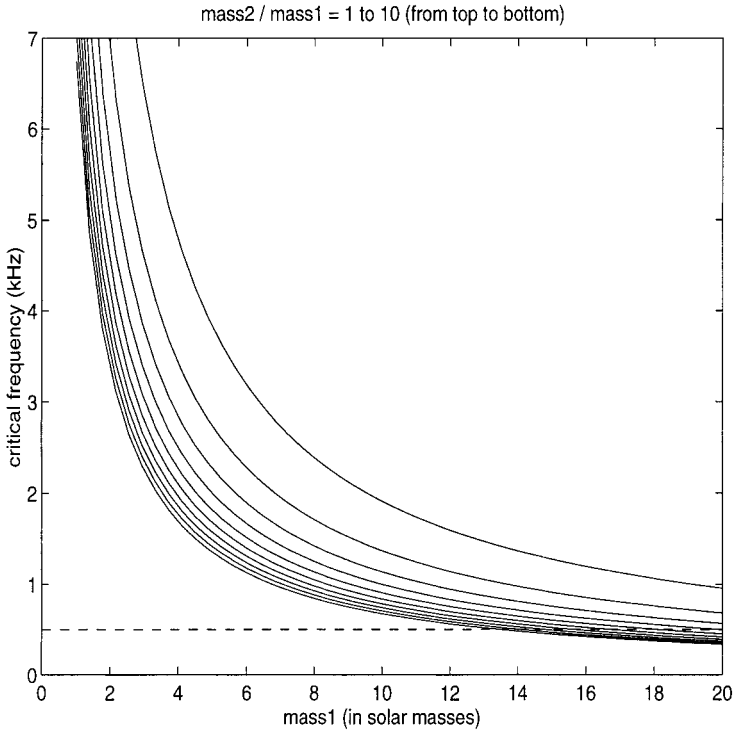

FIG. 1. Qualitative validity of the chirp interpretation for gravitational waves. Gravitational waves radiated by coalescing binaries can be considered as chirps as long as their maximum frequency in much smaller than a critical frequency which depends on the masses m_1 and m_2 of the binary. This diagram plots (solid lines) this critical frequency when m_1 varies between $1M_\odot$ and $10M_\odot$, and when $m_2 = km_1$, with $1 \leq k \leq 10$. The dotted line (plotted here arbitrarily at 500 Hz) stands for the high-frequency cutoff of the detector, which allows one to get a rough bound for the validity of the approximation.

and the condition (11) defines, in turn, a frequency interval characterized by

$$f \ll f_c = f_x(t_c) = 100 \times (1600\pi)^{3/5}\mathcal{M}_\odot^{-1} \approx 1.66 \times 10^4 \mathcal{M}_\odot^{-1}. \tag{12}$$

Figure 1 illustrates the validity of this condition when m_1 varies between $1M_\odot$ and $10M_\odot$, and when $m_2 = km_1$, with $1 \leq k \leq 10$. It follows from this diagram that, in the case where the high-frequency cutoff of the detector is supposed to be about 500 Hz, the chirp interpretation can be considered as valid for a wide range of scenarios which are likely to be observed.

Considering (10) as a chirp, its frequency spectrum can be obtained by means of a stationary phase approximation, leading to the following result:

PROPOSITION 9. *In the domain where it can be considered as a chirp, the waveform* (10) *corresponds approximately to a* power-law chirp *in the sense of Definition* 6, *with an envelope index* $r = (\alpha - \beta/2)/(\beta - 1)$, *a phase index* $k = \beta/(\beta - 1)$, *a phase shift* $\gamma = \pi/4$, *a chirp rate*

$$c = -\frac{\beta - 1}{\beta}(d\beta)^{-1/(\beta-1)}, \tag{13}$$

and an amplitude

$$C = \frac{A}{\sqrt{|\beta - 1|}}(d\beta)^{(\alpha-1/2)/(\beta-1)}. \tag{14}$$

The relative error in this approximation is frequency dependent and is bounded by

$$Q(f) = \frac{5}{4}\left(\frac{\alpha^2}{\beta - 1} + \alpha + \frac{(\beta - 2)(\beta - 1/2)}{6}\right)\left(\frac{d}{\beta}\right)^{1/(\beta-1)} f^{-\beta/(\beta-1)}. \tag{15}$$

Proof. Computing the Fourier spectrum of (10) amounts to evaluating the integral

$$X(f; t_0, d) = e^{-i2\pi f t_0}\int_0^{+\infty} a(t)e^{i\psi(t)}dt, \tag{16}$$

with $a(t) = At^{-\alpha}$ and $\psi(t) = -2\pi(dt^{\beta} - ft)$.

It is clear that $\psi(t)$ has no stationary point when $f < 0$ and, following the result of Appendix A, we can first conclude that (10) is almost analytic, as long as the chirp condition (11) is satisfied.

For positive frequencies, $\psi(t)$ has one and only one nondegenerate stationary point, namely

$$t_s = \left(\frac{f}{d}\right)^{1/(\beta-1)},$$

with the condition $\ddot{\psi}(t_s) > 0$.

When specializing to the model (10) the general result (23), it turns out that (16) exactly coincides with a power-law chirp in the sense of Definition 6, with the constants given in (13) and (14). For each frequency, the stationary phase evaluation of the spectrum amounts to considering the signal contribution at $t = t_s$, and thus the remainder (24) at this point. After a careful removal of all indeterminancies associated with the evaluation of $Q(t_s)$, we finally get the frequency-dependent result given in (15), which allows one to bound the frequency domain over which the stationary phase approximation can be considered as valid, given a maximum relative error.

Two remarks can be made at this point. First, whereas "chirp conditions" of Definition 1 are usually advocated for validating stationary phase approximations (see, e.g., [11, 30] or [10]), the validity of the approximation is in fact controlled by (24) and this happens to be much more intricate. Second, if we apply the above result (15) to the case of gravitational waves, we get that, for the relative error in the stationary phase approximation to be at most x percent, frequency must be bounded by

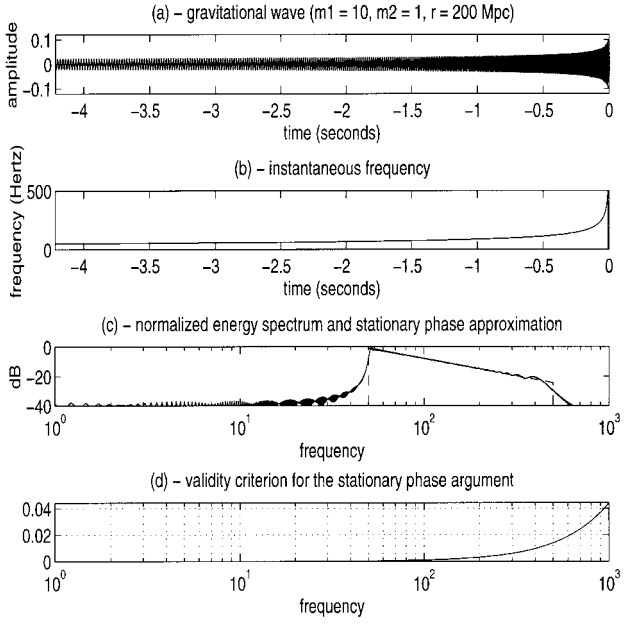

FIG. 2. Stationary phase approximation for the spectrum of a gravitational wave. The waveform, expected to be radiated by a coalescing binary composed of two objects of 1 $M_\odot$ and $10M_\odot$ at a distance of 200 Mpc, is plotted in (a), with the corresponding instantaneous frequency in (b). The energy spectral density is given in (c) (solid line), along with the stationary phase approximation (dashed line). The validity of this approximation is controlled by the frequency-dependent relative error plotted in (d).

$$f \leq 7.18 \times 10^4 x^{3/5} \mathcal{M}_\odot^{-1}. \tag{17}$$

in agreement with the qualitative chirp condition given in (12). Therefore, both the heuristic and the exact criteria turn out to be of the same nature, but the results of Proposition 9 allow for a quantitative control of the approximation.

Figure 2 presents a typical example of a waveform and illustrates the effectiveness of the stationary phase approximation.

6.2. A Simplified Time-Frequency Detector

Strictly speaking, the optimum time–frequency detector (7) requires one to compute a filtered version (in time) of the Bertrand distribution of the observation. This involves, unfortunately, a very heavy computational burden and, in order to end up with a feasible solution, it is mandatory to consider simpler, yet accurate, time–frequency descriptions instead of the exact function $\rho_R(t, f)$ given in (8). Whereas such a simplification may not be possible in the general case, it turns out that it can be effectively achieved in the specific case of gravitational waves, thanks to the specific values of the physical parameters which are involved.

In fact, if we come back to (8), we can write in an equivalent way

$$\int_{-\infty}^{+\infty} \rho_R(t, f) e^{-i2\pi\xi t} dt = C^2 f^{2r+1-q} h(u) \int_{-\infty}^{+\infty} P_R^{(k)}(t, f) e^{-i2\pi\xi t} dt \tag{18}$$

with

$$h(u) = \frac{(\lambda_k(u)\lambda_k(-u))^{r+1}}{\dot{\zeta}_k(u)} A(f\lambda_k(u)) A(f\lambda_k(-u)) \tag{19}$$

and

$$u = \zeta_k^{-1}\left(\frac{\xi}{f}\right).$$

Due to low-frequency (seismic noise) and high-frequency (photon noise) limitations, the effective observation bandwidth is necessarily restricted to some bandpass frequency interval $f_- \le f \le f_+$ (with typical values that we can choose to be $f_- \approx 50$ Hz and $f_+ \approx 500$ Hz). This has for consequence that the Fourier spectrum

$$\int_{-\infty}^{+\infty} P_R^{(k)}(t, f) e^{-i2\pi\xi t} dt = f^{2r+1-q} (\lambda_k(u)\lambda_k(-u))^{r+1} R(f\lambda_k(u)) \overline{R(f\lambda_k(-u))}$$

is nonzero only in the range

$$|u| \le u_+ = \log \frac{f_+}{f_-},$$

and it follows that the u-dependent prefactor $h(u)$ of the Fourier transform of $P_R^{(k)}(t, f)$ can be ignored in (18) as long as it is almost equal to 1 for $|u| \le u_+$.

Within the above-mentioned frequency band, we can consider (see, e.g., [20, 21]) that the power spectrum density $\Gamma_n(f)$ of the observation noise $n(t)$ has essentially a continuous background which behaves as $\Gamma_n(f) = \sigma^2 f^{-\epsilon}$, with $\epsilon \approx 1$.[3] Assuming therefore that

$$A(f) = \sigma^{-2} f^{\epsilon-(3r+2)}$$

for $f_- \le f \le f_+$, we get from (19) that

$$h(u) = \sigma^{-4} \frac{(\lambda_k(u)\lambda_k(-u))^{\epsilon-(2r+1)}}{\dot{\zeta}_k(u)}$$

for $|u| \le u_+$. In the case of coalescing binaries ($k = -\frac{5}{3}$, $r = \frac{1}{6}$) and "$1/f$" noise ($\epsilon = 1$), this reduces to

$$\sigma^4 h(u) = \frac{(\lambda_{-5/3}(u)\lambda_{-5/3}(-u))^{-1/3}}{\dot{\zeta}_{-5/3}(u)}, \tag{20}$$

[3] Let us notice that this is a first approximation and that, in the case of actual detectors, it will certainly have to be refined on the basis of more realistic noise models.

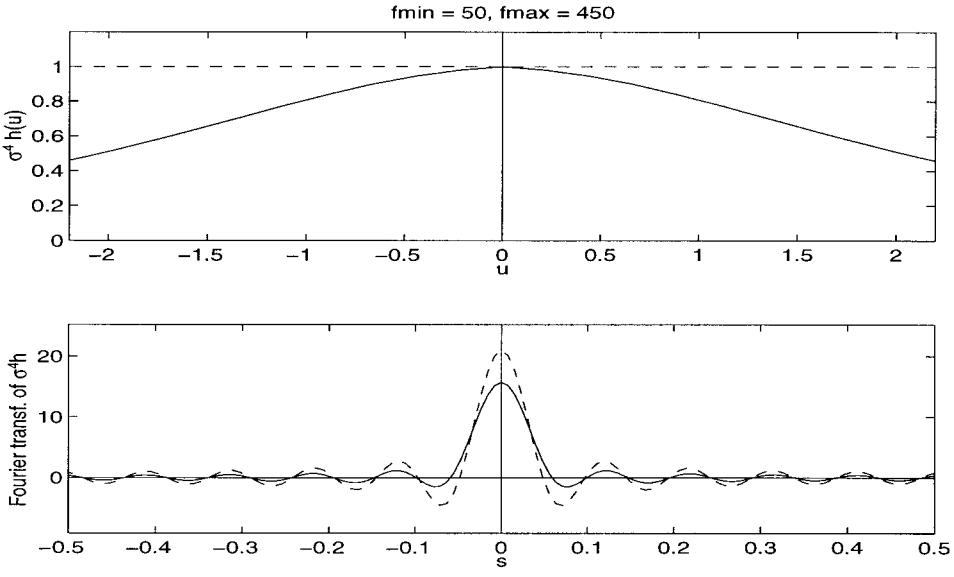

FIG. 3. When the frequency band of the detector is limited, the time–frequency function to be used can be well approximated by a Bertrand distribution provided that the function $\sigma^4 h(u)$, defined in (20), acts as a convolution unit in the space of u-limited functions. The validity of this approximation is illustrated here by plotting in the upper diagram $\sigma^4 h(u)$ (solid line) and the indicator function of the u-interval associated with the frequency range 50–450 Hz (dotted line), and by comparing in the lower diagram their Fourier transforms.

a quantity which, in the considered space of u-limited functions, can be considered as a convolution unit, as illustrated in Fig. 3.

When the above approximation is valid, it leads therefore to a detector as in (7), but with the simplification

$$\rho_R(t, f) \approx \frac{C^2}{\sigma^4} f^{q+2\epsilon-(4r+3)} P_R^{(k)}(t, f).$$

Given this simplified structure, the final problem reduces to finding some accurate and easy-to-compute approximation to the Bertrand distribution $P_R^{(k)}(t, f)$. Since the key feature of this distribution is to satisfy the perfect localization (6) on "matched" chirps, the solution that we propose is to replace it with a *reassigned spectrogram* [3, 5] $\check{S}_X^h(t, f)$ which, when applied to the same power-law chirps, is known to behave approximately as

$$\check{S}_{X_{r,k}}^h(t, f) \approx C^2 f^{-2(r+1)} \delta(t - t_X(f)). \tag{21}$$

The principle of reassignment is briefly recalled in Appendix B and the effectiveness of this approximation is illustrated in Fig. 4.

Comparing (6) and (21), we are led to choosing $q = 2r + 1$, with the final form of the approximated optimum detector given by

$$\Lambda^w(r; t, c) \approx \frac{C^2}{\sigma^4} \int_0^{+\infty} \check{S}_R^h(t + ckf^{k-1}, f) f^{2(\epsilon-(r+1))} df.$$

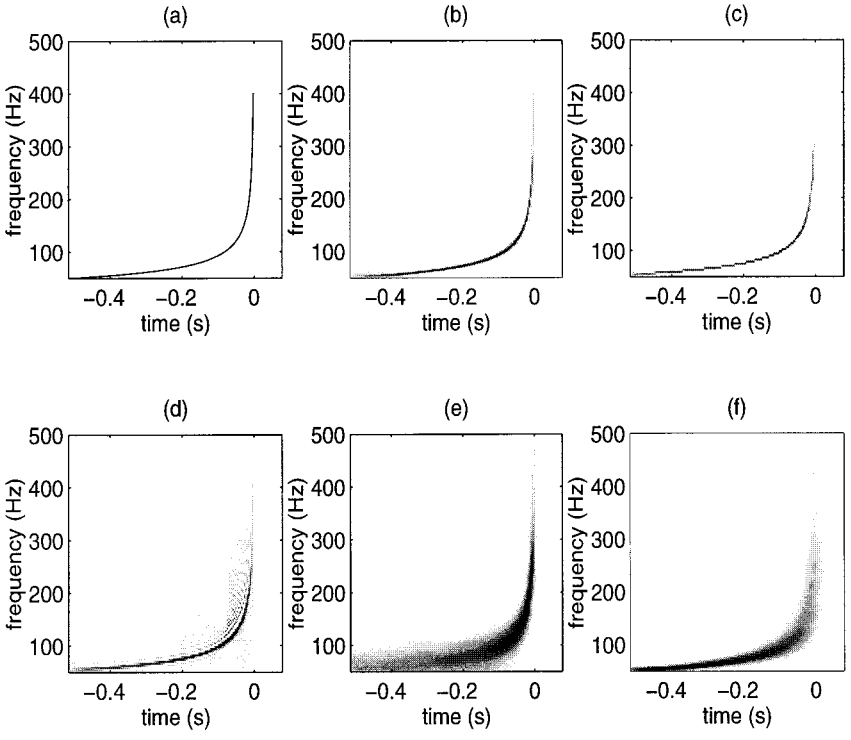

FIG. 4. Time–frequency distributions for gravitational waves. Given a gravitational wave radiated by a coalescing binary, a "matched" time–frequency distribution is expected to be as localized as possible along the instantaneous frequency curve. The "ideal" representation (a) is compared with a number of candidate distributions (coalescence time is fixed to $t_0 = 0$). From a theoretical point of view, it is known that the desired localization is guaranteed by using a matched Bertrand distribution ($k = -\frac{5}{3}$): this is illustrated in (b), where the algorithm described in [17] has been used. An effective and easy-to-compute approximation is given by the reassigned spectrogram (c). These two situations contrast with the more classical solutions provided by the Wigner–Ville distribution (d), the spectrogram (e), and the scalogram (f).

In the specific case of coalescing binaries, we can prefer to parameterize the signal to detect by means of its coalescence time t and reduced chirp mass $\mathcal{M}_\odot$. Together with the right constants, we finally get (up to an amplitude factor)

$$\Lambda^w(r;\, t,\, \mathcal{M}_\odot) \propto \int_{\mathcal{L}(t,\mathcal{M}_\odot)} \check{S}_R^h(\tau,\, f)\, f^{-2/3},$$

with

$$\mathcal{L}(t,\, \mathcal{M}_\odot) = \{(\tau,\, f) | t - \tau = 3 \times 100^{8/3} \mathcal{M}_\odot^{-5/3} f^{-8/3}\}.$$

6.3. An Illustration

In order to illustrate the effectiveness of the proposed approach, we present in Fig. 5 two different examples based upon one of the typical situations discussed in [20, 21]. Both

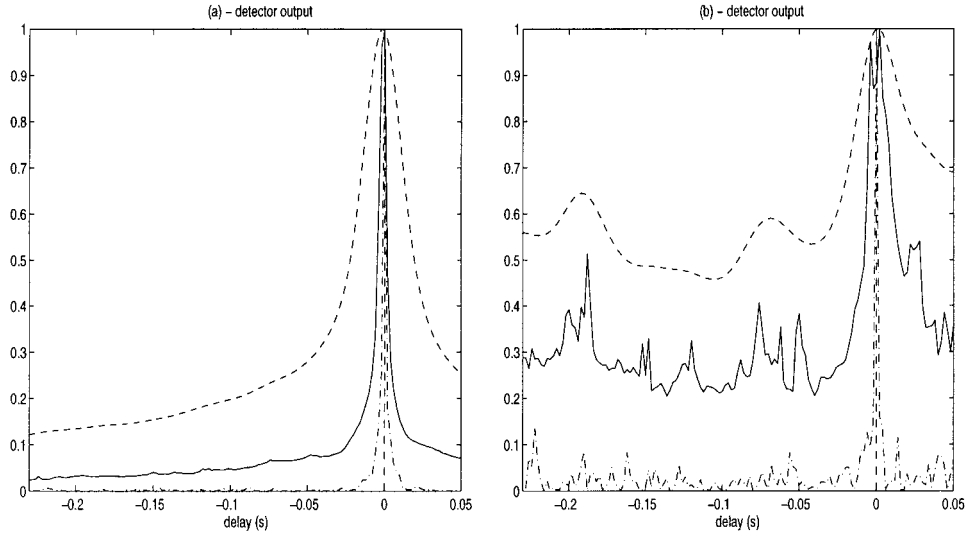

FIG. 5. Detection of a gravitational wave. This figure illustrates the efficiency of an optimum time–frequency-based detection for a gravitational wave with coalescence time $t = 0$ of a binary composed of two objects of $1M_\odot$ and $10M_\odot$ at a distance of 200 Mpc in case (a) and 1 Gpc in case (b). Since the distance between the binary and Earth changes the only signal amplitude, the signal-to-noise ratio is the only parameter that has been modified between these two examples. Each plot compares the squared envelope of the output of the matched filter (dashed–dotted line) with a time–frequency strategy based on a line integration over either a classical spectrogram (dashed line) or its reassigned version (solid line). In order to make appear more clearly what is gained in terms of contrast, the maximum of each of these curves has been arbitrarily normalized to unity.

examples will assume that the binary consists of two objects of $1M_\odot$ and $10M_\odot$ (coalescence time set to $t = 0$). The binary is located at a distance of 200 Mpc from Earth in the first example, and 1 Gpc in the second one. The simulation was run by corrupting the data with Gaussian additive noise, with $\epsilon = 1$ and $\sigma^2 = 0.7 \times 10^{-42}$/Hz over a frequency range of 50–500 Hz. The proposed strategy, based on the reassigned spectrogram, does not reach the ideal performance predicted by the matched filter theory, because of the limited accuracy of the different approximations which have been involved in its derivation (in particular, the band-limited nature of the signal implies that the Bertrand distribution cannot be perfectly localized along the group delay curve). However, the figure shows that this strategy clearly allows for the detection of the chirp and that it also overperforms a crude path integration based on a standard spectrogram.

In the examples of Fig. 5, the chirp mass $\mathcal{M}_\odot$ was implicitly assumed to be known, which is by no means the case in practice. Assuming that $\mathcal{M}_\odot$ is unknown, a refined strategy amounts to applying the previous one in parallel by performing as many line integrations as is necessary for sampling values of $\mathcal{M}_\odot$ over some expected range. Figures 6 and 7 exhibit the application of this strategy on the reassigned spectrogram and standard spectrogram, respectively. This joint detection–estimation problem allows also for an estimate of $\mathcal{M}_\odot$ to be obtained. It should be noted that, when scanning test values for $\mathcal{M}_\odot$, the reference signal energy is modified. The output of each detector therefore must be divided by a factor proportional to the squared amplitude of the reference signal (which varies as $\mathcal{M}_\odot^{5/3}$) in order to compare coherent results.

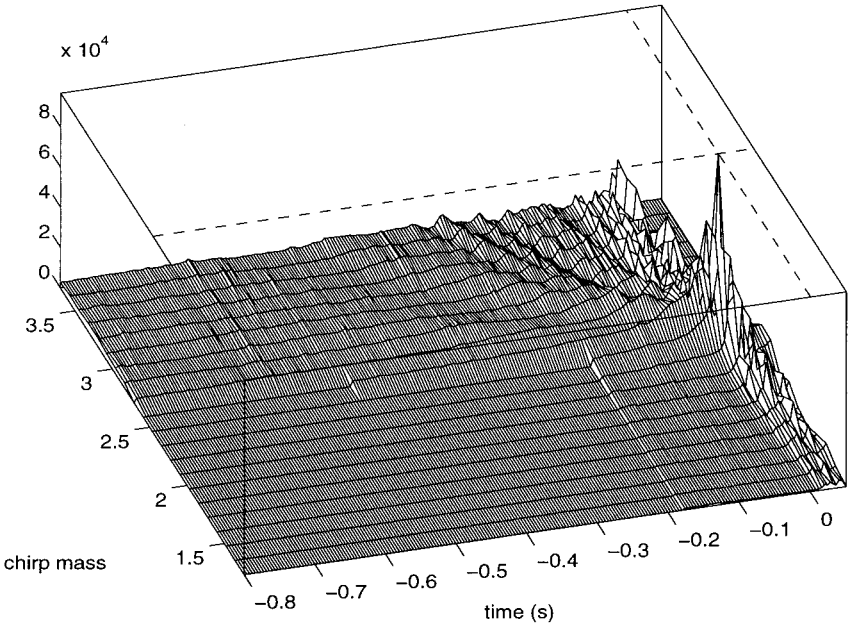

FIG. 6. Joint detection–estimation for gravitational waves based on the reassigned spectrogram. In the case where the chirp mass parameter $\mathcal{M}_\odot$ is unknown, different line integrations (similar to those of Fig. 5, but over a number of different time–frequency curves) have to be performed, here on the reassigned spectrogram. This results in a surface whose maximum allows for the detection of the gravitational wave (when it exceeds some prescribed threshold) and for the estimation of both the time of coalescence and the chirp mass (actual values are indicated with dashed lines).

7. CONCLUSION

The purpose of this paper was to combine elements from optimum detection theory and time–frequency analysis so as to provide a coherent framework for intuitive strategies aimed at detecting chirplike signals by some line integration in the time–frequency plane. The example of gravitational waves (expected to be radiated by coalescing binaries) is particularly important in this respect, and the possibility of their time–frequency detection was discussed in some detail. Once the conditions for such an alternative quasi-optimum strategy have been established, the question now is to discuss further what can be really gained from such a new approach, especially in terms of versatility and robustness.

APPENDIX A: THE STATIONARY PHASE METHOD

Let I be an integral of the form

$$I = \int_\Omega a(t) e^{i\psi(t)} dt, \tag{22}$$

where both $a(t) > 0$ and $\psi(t)$ are C^1, whereas $\mathrm{supp}\{a(t)\}$ is restricted to some interval Ω of the real line over which $a(t)$ is integrable.

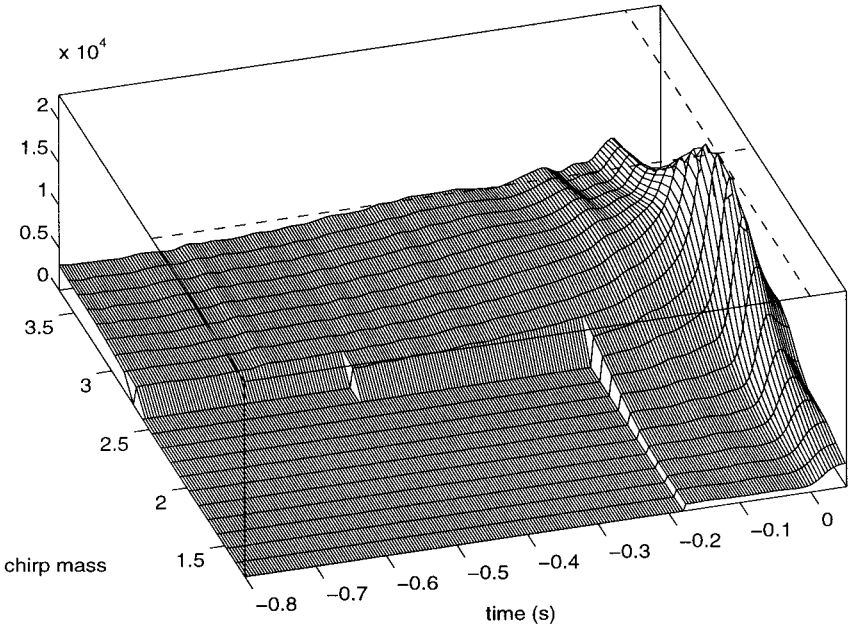

FIG. 7. Joint detection–estimation for gravitational waves based on the spectrogram. The surface shown here is the response of the detector–estimator based on path integrations of the standard spectrogram. This should be compared with the one in Fig. 6. The smoothness of the detection peak and the poor contrast between its maximum and the noise level make the detection procedure more difficult. Dashed lines indicated actual values of the time of coalescence and the chirp mass.

Assuming that the amplitude $a(t)$ is slowly varying as compared to the oscillations of the phase $\psi(t)$, (22) corresponds to an oscillatory integral. Using standard arguments, we can therefore heuristically consider that, when integrated, positive and negative contributions of fast oscillations tend to cancel each other, with the consequence that the main contribution to (22) only comes from the vicinity of those points where oscillations are significantly slowed down, i.e., where the derivative of the phase is zero. This is the essence of the stationary phase principle.

In the specific case of the model (22), classical results from stationary phase theory (as presented, e.g., in [33]) cannot be directly applied, because phase oscillations are not controlled by a multiplicative parameter becoming arbitrarily large. Nevertheless, if we assume that $\psi(t)$ has one and only one nondegenerate stationary point t_s (i.e., that $\dot{\psi}(t_s) = 0$ and $\ddot{\psi}(t_s) \neq 0$), we can (following, e.g., [19, 35]) make the change of variables

$$u^2 = \frac{\psi(t) - \psi(t_s)}{\ddot{\psi}(t_s)/2}$$

so as to rewrite (22) in the form

$$I = e^{i\psi(t_s)} \int_{\Omega'} g(u) e^{i\beta u^2} du,$$

with $g(u) = a(x(u))(du/dx)^{-1}$ and $\beta = \ddot{\psi}(t_s)/2$. Following [19], we get for such an expression a decomposition of the type $I = I_a + R$, where the first term corresponds to the stationary phase approximation

$$I_a = \sqrt{\frac{2\pi}{|\ddot{\psi}(t_s)|}}\, a(t_s) e^{i\psi(t_s)} e^{i(\mathrm{sgn}\,\ddot{\psi}(t_s))\pi/4}, \tag{23}$$

whereas the remainder R is such that

$$Q = \left|\frac{R}{I_a}\right| \leq Q_m = \frac{5}{4}\frac{\sup_{u\in\Omega'} |\ddot{g}|}{|\beta| g(t_s)}.$$

The stationary phase approximation is therefore valid if we have $Q_m \ll 1$. An explicit evaluation of this quantity leads to $Q_m = \sup_{t\in\Omega} Q(t)$, with

$$Q(t) = 5\sqrt{2|\ddot{\psi}(t_s)|}\left|\frac{a}{a(t_s)}\frac{\psi^{1/2}}{\dot{\psi}}\right| \left|\frac{\ddot{a}}{a}\frac{\psi}{\dot{\psi}^2} + \frac{3}{2}\frac{\dot{a}}{a\dot{\psi}}\left(1 - \frac{\psi\ddot{\psi}}{\dot{\psi}^2}\right) + \left(3\psi\left(\frac{\ddot{\psi}}{\dot{\psi}^2}\right)^2 - \frac{3}{2}\frac{\ddot{\psi}}{\dot{\psi}^2} - \frac{\psi\psi'''}{\dot{\psi}^3}\right)\right|, \tag{24}$$

where ψ denotes the function $\psi(t) - \psi(t_s)$ for short.

The above closed form expression for the remainder allows one both to make explicit the conditions under which (23) is a valid approximation for (22) and to bound the corresponding error.

In the case where there is no stationary point, it is intuitive that the integral (22) should tend to zero as oscillations become faster. To make this point more precise, let us assume that $\dot{\psi}(t) \neq 0$ for any $t \in \Omega$, so that we can rewrite (22) as

$$I = \int_\Omega \frac{a(t)}{i\dot{\psi}(t)}\, i\dot{\psi}(t) e^{i\psi(t)} dt.$$

An integration by parts leads to

$$I = \frac{a(t)}{i\dot{\psi}(t)}\, e^{i\psi(t)}\Big|_{\partial\Omega} + i\int_\Omega a(t)\left[\frac{\dot{a}(t)}{a(t)\dot{\psi}(t)} - \frac{\ddot{\psi}(t)}{\dot{\psi}^2(t)}\right] e^{i\psi(t)} dt,$$

from which it follows that

$$|I| \leq \left|\frac{a(t)}{\dot{\psi}(t)}\right|_{\partial\Omega} + \left(\left\|\frac{\dot{a}(t)}{a(t)\dot{\psi}(t)}\right\|_\infty + \left\|\frac{\ddot{\psi}(t)}{\dot{\psi}^2(t)}\right\|_\infty\right)\int_\Omega |a(t)| dt.$$

Assuming that the amplitude may be regularized so as to make negligible the first term, we get that

$$\frac{|I|}{\|a\|_1} \leq \left\| \frac{\dot{a}(t)}{a(t)\dot{\psi}(t)} \right\|_\infty + \left\| \frac{\ddot{\psi}(t)}{\dot{\psi}^2(t)} \right\|_\infty .$$

This result can be interpreted the following way: as compared to the situation where the oscillations of the phase would be infinitely slowed down, the absolute value of the oscillatory integral (22) with no stationary point is bounded by a quantity whose decay to zero is controlled by chirplike conditions.

In the case we are here mainly interested in (i.e., the evaluation of a Fourier transform), we have $\psi(t) = \varphi(t) - 2\pi ft$, where $\varphi(t)$ is the phase of a chirp. Since we have $\dot{\varphi}(t) > 0$ for any $t \in \Omega$, we can conclude that the frequency domain for which no stationary point exists is the half-line of negative frequencies. Since we have futhermore $\ddot{\psi}(t) = \ddot{\varphi}(t)$ and $\dot{\psi}(t) \geq \dot{\varphi}(t)$ when $f < 0$, we get that

$$\left\| \frac{\dot{a}(t)}{a(t)\dot{\psi}(t)} \right\|_\infty \leq \left\| \frac{\dot{a}(t)}{a(t)\dot{\varphi}(t)} \right\|_\infty$$

and

$$\left\| \frac{\ddot{\psi}(t)}{\dot{\psi}^2(t)} \right\|_\infty \leq \left\| \frac{\ddot{\varphi}(t)}{\dot{\varphi}^2(t)} \right\|_\infty .$$

This proves that the chirp conditions of Definition 1 are sufficient to guarantee the quasi-analyticity of the exponential model (1), in the sense that spectral contributions at negative frequencies are negligible.

APPENDIX B: THE REASSIGNMENT METHOD

The spectrogram $S_X^h(t, f) = |F_X^h(t, f)|^2$, i.e., the squared modulus of the short-time Fourier transform $F_X^h(t, f) = \int_{-\infty}^{+\infty} X(\xi) H^*(\xi - f) e^{i2\pi(\xi - f)t} d\xi$, can also be viewed as a smoothed version of the Wigner–Ville distribution of the signal

$$S_X^h(t, f) = \int \int_{-\infty}^{+\infty} W_x(s, \xi) W_h(s - t, \xi - f) ds d\xi.$$

The purpose of reassignment [24] is to refocus the spectrogram on the time–frequency energy content given by the Wigner–Ville distribution. It basically consists in moving the values of the spectrogram from their initial computation point to a time–frequency location $(\hat{t}(t, f), \hat{f}(t, f))$ given by a local center of mass computed over the Wigner–Ville distribution of the signal

$$\check{S}_X^h(t, f) = \int \int_{-\infty}^{+\infty} S_X^h(s, \xi) \delta(t - \hat{t}(s, \xi), f - \hat{f}(s, \xi)) ds d\xi.$$

This results in a squeezing of each signal component along its associated group delay and/or instantaneous frequency path. For example, the reassigned spectrogram is perfectly localized on linear chirps with a constant envelope,

$$x(t) = \exp\left\{ i2\pi\left(\frac{\alpha}{2}\, t^2 + \beta t + \gamma\right)\right\} \Rightarrow \check{S}_X^h(t, f) = \delta(f - (\alpha t + \beta)).$$

In the case of nonlinear chirps, a similar squeezing effect will be obtained provided that the instantaneous frequency or the group delay of the signal is almost linear *locally*, i.e., in a time–frequency domain whose effective support is defined by the time and frequency widths of the analysis window. One can mention that reassignment has been proved not to be restricted to the spectrogram and its application has been extended [3] to all smoothed distributions within Cohen and affine classes.

From a computational viewpoint, reassignment is supported by efficient algorithms. In the case of the spectrogram, we get explicitly [3]

$$\begin{aligned} \hat{t}(t, f) &= t + \mathrm{Re}\,\{F_X^u(t, f)/F_X^h(t, f)\} \\ \hat{f}(t, f) &= f - \mathrm{Im}\,\{F_X^v(t, f)/F_X^h(t, f)\}, \end{aligned} \tag{25}$$

where $u(t) = th(t)$ and $v(t) = dh/dt$. Therefore, the resulting algorithm combines, in a proper way, three STFTs of the signal based on three distinct windows (and even two only if the window is a Gaussian).

REFERENCES

1. M. Abramowitz and I. Stegun, "Handbook of Mathematical Functions with Formulas, Graphs and Mathematical Tables," Dover, New York, 1972.
2. R. A. Altes, Detection, estimation and classification with spectrograms, *J. Acoust. Soc. Amer.* **67** (1980), 1232–1246.
3. F. Auger and P. Flandrin, Improving the readability of time-frequency and time-scale representations by reassignment methods, *IEEE Trans. Signal Process.* **SP-43** (1995), 1068–1089.
4. S. Barbarossa, Analysis of multicomponent LFM signals by a combined Wigner–Hough transform, *IEEE Trans. Signal Process.* **SP-43** (1995).
5. S. Barbarossa and O. Lemoine, Analysis of nonlinear FM signals by pattern recognition of their time-frequency representation, *IEEE Signal Process. Lett.* **SPL-3** (1996), 112–115.
6. J. Bertrand and P. Bertrand, A class of affine Wigner distributions with extended covariance properties, *J. Math. Phys.* **33** (1992), 2515–2527.
7. J. Bertrand and P. Bertrand, Some practical aspects of the affine time-frequency distributions, *in* "Proc. 13th Conference GRETSI," pp. 25–28, Juan-Les-Pins, France, 1991.
8. G. Boudreaux-Bartels, Mixed time-frequency signal transformations, *in* "The Transforms and Applications Handbook" (A. D. Poularikas, Ed.), CRC Press, Boca Raton, FL, 1996.
9. L. Cohen, "Time-Frequency Analysis," Prentice Hall, Englewood Cliffs, NJ, 1995.
10. N. Delprat, B. Escudié, Ph. Guillemain, R. Kronland-Martinet, Ph. Tchamitchian, and B. Torrésani, Asymptotic wavelet and Gabor Analysis: Extraction of instantaneous frequencies, *IEEE Trans. Inform. Theory* **38** (1992), 644–664.

11. L. S. Finn and D. F. Chernoff, Observing binary inspiral in gravitational radiation: One interferometer, *Phys. Rev. D* **47** (1993), 2198–2219.
12. P. Flandrin, On detection-estimation procedures in the time-frequency plane, *in* "Proc. IEEE Int. Conf. on Acoust., Speech and Signal Proc.," pp. 2331–2334, Tokyo, 1986.
13. P. Flandrin, A time-frequency formulation of optimum detection, *IEEE Trans. Acoust. Speech Signal Process.* **ASSP-36** (1988), 1377–1384.
14. P. Flandrin, "Temps-Fréquence," Hermès, Paris, 1993.
15. P. Flandrin and P. Gonçalvès, From wavelets to time-scale energy distributions, *in* "Recent Advances in Wavelet Analysis" (L. L. Schumaker and G. Webb, Eds.), pp. 309–334, Academic Press, Boston, 1994.
16. P. Flandrin and P. Gonçalvès, Geometry of affine time-frequency distributions, *Appl. Comput. Harmon. Anal.* **3** (1996), 10–39.
17. P. Gonçalvès and R. G. Baraniuk, A pseudo-Bertrand distribution for time-scale analysis, *IEEE Signal Process. Lett.* **3** (1996), 82–84.
18. I. S. Gradshteyn and I. M. Ryzhik, "Tables of Integrals, Series and Products," Academic Press, New York, 1980.
19. J. Harthong, Études sur la Mécanique Quantique, *Astérisque* (1984), 7–26.
20. J.-M. Innocent and B. Torrésani, A multiresolution strategy for detecting gravitational waves generated by binary coalescence, Internal Report CPT-96/P.3379, CPT-CNRS, Marseille, 1996.
21. J.-M. Innocent and B. Torrésani, Wavelets and binary coalescences detection, *Appl. Comput. Harmon. Anal.* **4** (1997), 113–116.
22. S. Jaffard and Y. Meyer, Wavelet methods for pointwise regularity and local oscillations of functions, *Mem. Amer. Math. Soc.* **123** (1996), 587.
23. A. J. E. M. Janssen, On the locus and spread of pseudo-density functions in the time-frequency plane, *Philips J. Res.* **37** (1982), 79–110.
24. K. Kodera, C. De Villedary, and R. Gendrin, A new method for the numerical analysis of nonstationary signals, *Phys. Earth Plan. Int.* **12** (1976), 142–150.
25. S. M. Kay and G. F. Boudreaux-Bartels, On the optimality of the Wigner distribution for detection, *in* "Proc. IEEE Int. Conf. on Acoust., Speech and Signal Proc.," pp. 1017–1020, Tampa, 1985.
26. S. D. Mohanty and S. V. Dhurandhar, Hierarchical search strategy for the detection of gravitational waves from coalescing binaries, *Phys. Rev. D* **54** (1996), 7108–7128.
27. F. Oberhettinger, "Fourier Transforms of Distributions and Their Inverses—A Collection of Tables," Academic Press, New York, 1973.
28. A. Papandreou, S. M. Kay, and G. F. Boudreaux-Bartels, The use of hyperbolic time-frequency representations for optimum detection and parameter estimation of hyperbolic chirps, *in* "Proc. IEEE Int. Symp. on Time-Frequency and Time-Scale Analysis," pp. 369–372, Philadelphia, 1994.
29. B. Picinbono, On instantaneous amplitude and phase of signals, *IEEE Trans. Signal Process.* **SP-45** (1997), 552–560.
30. B. S. Sathyaprakash and S. V. Dhurandhar, Choice of filters for the detection of gravitational waves from coalescing binaries, *Phys. Rev. D* **44** (1991), 3819–3834.
31. A. M. Sayeed and D. L. Jones, Optimal detection using bilinear time-frequency and time-scale representations, *IEEE Trans. Signal Process.* **SP-43** (1995), 2872–2883.
32. B. F. Schutz, Gravitational wave sources and their detectability, *Classical Quantum Gravity* **6** (1989), 1761–1780.
33. E. M. Stein, "Harmonic Analysis," Princeton Univ. Press, Princeton, 1993.
34. K. S. Thorne, Gravitational radiation, *in* "300 Years of Gravitation" (S. W. Hawking and W. Israel, Eds.), pp. 330–458, Cambridge Univ. Press, Cambridge, 1987.
35. B. Torrésani, "Analyse Continue par Ondelettes," InterÉditions/CNRS Éditions, Paris, 1995.
36. A. Unterberger, The calculus of pseudo-differential operators of Fuchs type, *Comm. Partial Differential Equations* **9** (1984), 1179–1236.
37. A. D. Whalen, "Detection of Signals in Noise," Academic Press, San Diego, 1971.